

AD-A146 853

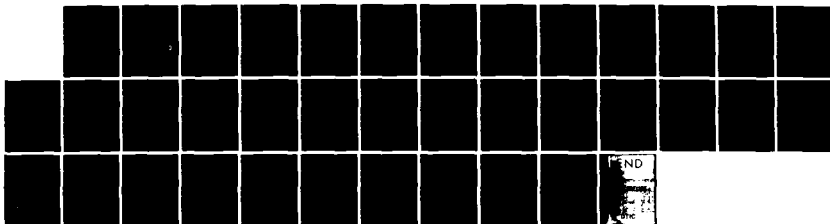
AN INVESTIGATION OF MEMBRANE-ENCAPSULATED TRYPA NOCIDES  
(U) WASHINGTON UNIV SEATTLE K J HAWANG 02 SEP 82  
DAMD17-78-C-8049

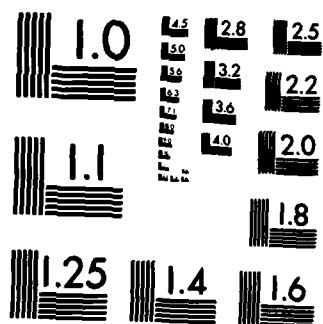
171

UNCLASSIFIED

F/G 6/15

NL





AD-A146 853

DTIC FILE COPY

(1)

AD \_\_\_\_\_

ARMY 011581-A-04

AN INVESTIGATION OF MEMBRANE-ENCAPSULATED TRYPANOCIDES

FINAL REPORT

KARL J. HWANG

SEPTEMBER 2, 1982

Supported by

U. S. ARMY MEDICAL RESEARCH AND DEVELOPMENT COMMAND  
Fort Detrick, Frederick, Maryland 21701

Contract No. DAMD 17-78-C-8049

University of Washington  
Seattle, Washington 98195

DTIC  
ELECTE  
OCT 16 1984  
S D B

Approved for public release; distribution unlimited.

The findings in this report are not to be construed as an official  
Department of the Army position unless so designated by other author-  
ized documents.

84 10 12 171

REPORT DOCUMENTATION PAGE		READ INSTRUCTIONS BEFORE COMPLETING FORM
1. REPORT NUMBER	2. GOVT ACCESSION NO. <b>A146 883</b>	3. RECIPIENT'S CATALOG NUMBER
4. TITLE (and Subtitle)  An Investigation of Membrane-Encapsulated Trypanocides		5. TYPE OF REPORT & PERIOD COVERED Final Report July 2, 1978-Dec. 31, 1981
7. AUTHOR(s) Karl J. Hwang		6. PERFORMING ORG. REPORT NUMBER ARMY 0115A1-A-04
9. PERFORMING ORGANIZATION NAME AND ADDRESS University of Washington Seattle, Washington 98195		8. CONTRACT OR GRANT NUMBER(s) DAMD17-78-C-8049
11. CONTROLLING OFFICE NAME AND ADDRESS US Army Medical Research and Development Command Fort Detrick, Frederick, Maryland 21701		10. PROGRAM ELEMENT, PROJECT, TASK AREA & WORK UNIT NUMBERS 62770A.3M162770A871.AF.070
14. MONITORING AGENCY NAME & ADDRESS (if different from Controlling Office)		12. REPORT DATE September 2, 1982
		13. NUMBER OF PAGES 36
		15. SECURITY CLASS. (of this report) Unclassified
		15a. DECLASSIFICATION/DOWNGRADING SCHEDULE
16. DISTRIBUTION STATEMENT (of this Report)  This document has been approved for public release and sale; its distribution is unlimited.		
17. DISTRIBUTION STATEMENT (of the abstract entered in Block 20, if different from Report)		
18. SUPPLEMENTARY NOTES		
19. KEY WORDS (Continue on reverse side if necessary and identify by block number)  Trypanosomiasis/Liposomes/Drug Carriers/ Lysosomal Degradation		
20. ABSTRACT (Continue on reverse side if necessary and identify by block number)  This progress report describes our research in studying the <u>in vivo</u> properties of liposomes as a potential drug carrier for trypanocidal agents. The report contains four sections. The first section describes a new method to load high levels of In-111 to liposomes, using 8-hydroxyquinidine and/or acetylacetone. The second section is a report of the finding of a large volume of distribution of sphingomyelin/cholesterol small unilamellar liposomes and their ability to get out of the vascular bed of a mouse. The third section discusses the		

Block 20 (Abstract) continued:

determination of the in vivo rate of release of liposome-entrapped In-111 in the liver and the influence of the liposomal size on the release. The fourth section describes the effect of lipid dose on the rate of the elimination of the long-lived sphingomyelin/cholesterol small unilamellar liposomes.

AD \_\_\_\_\_

ARMY 011581-A-04

AN INVESTIGATION OF MEMBRANE-ENCAPSULATED TRYPANOCIDES

FINAL REPORT

KARL J. HWANG

SEPTEMBER 2, 1982

Supported by

U. S. ARMY MEDICAL RESEARCH AND DEVELOPMENT COMMAND  
Fort Detrick, Frederick, Maryland 21701

Contract No. DAMD 17-78-C-8049

University of Washington  
Seattle, Washington 98195

Approved for public release; distribution unlimited.

The findings in this report are not to be construed as an official Department of the Army position unless so designated by other authorized documents.

## SUMMARY

This progress report describes our research in studying the disposition and degradation of liposomes in mice. The research programs were directed toward four related areas: (1) the development of methods to load high levels of radioactive cations to liposomes, (2) the investigation of the volume of distribution and transcapillary passage of small unilamellar liposomes, (3) the determination of the in vivo rate of release of liposome-entrapped  $^{111}\text{In}^{3+}$  from liposomes in tissue, and (4) the search for liposomes with a long half-life of blood clearance. Using 8-hydroxyquinoline or acetylacetone, we were able to load high levels of  $^{111}\text{In}^{3+}$  or  $^{67}\text{Ga}^{3+}$  to liposomes with 90% encapsulation efficiency. Using bovine brain sphingomyelin/cholesterol (2/1; mol/mol) small unilamellar liposomes (about 200 Å in diameter), we found that initially the small liposomes remained in the vascular system with a volume distribution of approximately 1.28 times larger than that of erythrocytes in the vascular system of mice. However, the small liposomes could get out of the vascular system of mice and were taken up by surrounding tissues over a period of 24 hours. Using the technique of gamma ray perturbed angular correlation and the method of loading In-111 to liposomes using 8-hydroxyquinoline, we found that the in vivo degradation rate of the outermost lipid bilayer of sphingomyelin/cholesterol (2/1; mol/mol) small liposomes is twice as slow as that of the large liposomes. Using bovine brain sphingomyelin and cholesterol at 2:1 molar ratio as the composition of liposomes, we found that the small unilamellar liposomes ( $187 \pm 42$  Å in diameter) remained intact in circulating blood of mice for at least one day and had the longest half-life (17 hours) in the blood ever reported in the literature for liposomes of natural sources.

# FORWARD

In conducting the research described in this report, the investigators adhered to the "Guide for Laboratory Animal Facilities and Care," as promulgated by the Committee on the Guide for Laboratory Animal Resources, National Academy of Sciences-National Research Council.



Accession For	
NTIS GRA&I	<input checked="" type="checkbox"/>
DTIC TAB	<input type="checkbox"/>
Unannounced	<input type="checkbox"/>
Justification	
By _____	
Distribution/	
Availability Codes	
Dist	Avail and/or Special
A-1	



# TABLE OF CONTENTS

	<u>Page</u>
I. Development of methods to load high levels of radioactive cations to liposomes . . . . .	7
II. Volume of distribution and transcapillary passage of small unilamellar liposomes. . . . .	8
III. Degradation of liposomes in mouse liver in vivo and in vitro. . .	10
IV. The long half-life of blood clearance of SM/CH (2/1; mol/mol) SUV in mice. . . . .	13
V. References . . . . .	14
VI. Figures and Tables . . . . .	15
VII. Glossary . . . . .	31
VIII. Distribution list. . . . .	33

## LIST OF FIGURES

- Figure 1. Dependence of the loading efficiency of (A)  $^{111}\text{In}^{3+}$  and (B)  $^{67}\text{Ga}^{3+}$  into DPPC small unilamellar liposomes on the concentration of oxine or oxine sulfate.
- Figure 2. Dependence of loading efficiency on concentration of acetylacetone used to introduce  $\text{In-}^{111}$  into small unilamellar SM/CH liposomes (2/1, mol/mol).
- Figure 3. Dependence of the loading efficiency of  $^{111}\text{In}^{3+}$  into DSPC/cholesterol (2/1; mol/mol) SUV on pH.
- Figure 4. Effect of citrate on the efficiency of loading  $^{111}\text{In}^{3+}$  to DPPC SUV.
- Figure 5. Clearance of SM/CH (2/1; mol/mol) SUV from the blood of mice.
- Figure 6. Blood clearance, liver uptake and the in vivo hepatic degradation of liposomes.
- Figure 7. In vitro degradation of SM/CH SUV in excised livers at two different temperatures.
- Figure 8. Degradation of the outermost shell of SM/CH bath-sonicated large multilamellar liposomes in the liver in vitro and in vivo.
- Figure 9. In vitro degradation of the outermost shell of SM/CH membrane extruded large multilamellar liposomes in two different livers.
- Figure 10. The clearance of SM/CH SUV from the blood of BALB/c mice at two typical liposome doses.
- Figure 11. The effect of liposome dose on blood clearance and liver uptake of SM/CH SUB at 23 hours post-injection.

### LIST OF TABLES

- Table 1. Tissue distributions of unilamellar sphingomyelin/cholesterol (2:1; Mol/Mol) liposomes intrapping  $^{67}\text{Ga}^{3+}$  by sonication and the same type of liposomes entrapping  $^{111}\text{In}^{3+}$  by  $^{111}\text{In}^{3+}$ -oxine loading in mice.
- Table 2. Time course of biodistribution of injected liposomal radioactivity in mice.
- Table 3. Calculated rate constants

This final progress report describes the findings of our study on the disposition and degradation of liposomes in mice during the period from July 1, 1978 to December 31, 1981. The research program was directed toward four major areas:

1) The development of methods to load high levels of radioactive cations to liposomes, (2) the investigation of the volume of distribution and transcapillary passage of small unilamellar liposomes, (3) the determination of the in vivo rate of release of liposome-entrapped  $^{111}\text{In}^{3+}$  from liposomes in tissue, and (4) the search for liposomes with a long half-life of blood clearance.

The research findings in these four related areas are summarized as follows:

#### I. Development of methods to load high levels of radioactive cations to liposomes.

The application of liposomes as potential carriers of pharmacological agents has been recognized increasingly in recent years. Before liposomes can be used successfully in humans, it is important to know the fate of liposomes in vivo. Liposomes encapsulating gamma-emitting radionuclides allow the study of the distribution of liposomes in vivo by non-invasive scintigraphic imaging. In addition, it has been demonstrated that by encapsulating an appropriate gamma-emitting radionuclide, such as  $^{111}\text{In}^{3+}$ , the change of the permeability of the lipid bilayer of liposomes to encapsulated materials in vivo can be estimated by the technique of gamma-ray perturbed angular correlation. To be able to investigate the fate of liposomes in vivo by the techniques of perturbed angular correlation and/or of gamma imaging, liposomes entrapping a high level of radioactivity are required. Current methods of encapsulating materials by bath or probe sonication produce liposomes entrapping only a low percentage of the starting materials. By using other methods of encapsulating, such as diethyl ether injection and reverse-phase evaporation the yield of entrapment can be increased. However, these procedures can only be used for the preparation of special types of liposomes. Thus, the development of a general and simple method of encapsulating a high level of gamma-emitting radionuclides in liposomes is highly desirable. The present report describes the application of 8-hydroxyquinoline (oxine), 8-hydroxyquinoline sulfate and acetylaceton for loading a high level of radioactivity of some useful radionuclides ( $^{67}\text{Ga}$ ,  $^{111}\text{In}$ ) into liposomes at room temperature.

The encapsulation of radioactive metallic cations, such as  $^{111}\text{In}^{3+}$  or  $^{67}\text{Ga}^{3+}$ , in the internal aqueous compartment of liposomes can be achieved with an efficiency of about 90%. The efficient loading of a high specific activity of cations into liposomes involves the transport of  $^{111}\text{In}^{3+}$  or  $^{67}\text{Ga}^{3+}$  through the lipid bilayer to an encapsulated strong chelate, such as nitrilotriacetic acid, by 8-hydroxyquinoline or acetylacetone, in conjunction with an efficient anion-exchange resin technique for the removal of the external cations. The efficiency of loading cations to liposomes is affected markedly by the concentration of 8-hydroxyquinoline (Fig. 1) or acetylacetone (Fig. 2), the pH of the final incubation mixture of liposomes and the complex of 8-hydroxyquinoline-metal (Fig. 3), and the presence of the chelating agents in the loading incubation mixture (Fig. 4). However, the loading efficiency is not affected by the pH of the internal aqueous compartment of liposomes over a range of pH 5-9, the concentration of the liposomes, the method of liposomal preparation, the lamellar structure of the liposomes, and the composition of liposomes. Furthermore, the

loading procedures do not appear to affect the size and the permeability of liposomes. There is a good agreement in the tissue distributions of the liposomes prepared by the present loading methods and those by the conventional method of encapsulation by sonication. (Table 1).

In conclusion, the anion-exchange resin, AG1K-8 (phosphate form), was found to be most efficient to remove external  $^{111}\text{In}^{3+}$  or  $^{67}\text{Ga}^{3+}$ . The most optimal condition for the loading procedure using oxine is to use 14-40 nmol oxine per ml for  $^{111}\text{In}^{3+}$ , and 2.1-2.8 nmol per ml for  $^{67}\text{Ga}^{3+}$ , in the incubation mixture of liposomes and oxine-metal in 5 mM acetate saline buffer at pH 5.5. The most optimal condition for the loading procedure using acetylacetone is to use 30 mM acetylacetone in 10 mM tris-buffered isotonic saline, pH 7.6. Detailed descriptions of the loading procedures have been published in two papers in *Biochim. Biophys. Acta* (1) and *J. Nucl. Med.* (2).

## II. Volume of distribution and transcapillary passage of small unilamellar liposomes.

In order to deliver drugs to tissues other than the RES using liposomes, two important criteria must be met in the design of liposomes. First, liposomes must be able to evade rapid uptake by the RES and stay in the circulating blood for an extended period of time to allow direction of the liposome to the desired tissues. Second, if homing molecules are attached to the liposomal surface, there should be sufficient interaction between the site-specific molecules (carbohydrates, or antibodies) on the surface of liposomes and receptors or antigens on the surface of the targeted cells. This suggests that in order for liposomes to be effective in delivering drugs to target tissues after intravenous administration, they must be able to pass out of the vascular system, allowing suitable contact or interaction with the target cells.

There are at least two ways to study whether and to what extent liposomes can pass out of the vascular system. The first approach, direct measurement of the amount of intact liposomes present in the extravascular space, requires analytical methods which differentiate the intact liposomes present in the extravascular space from the liposomal marker which is released from degraded liposomes and subsequently transported to the extravascular space. An alternative approach is to study the time course of the biodistribution of the liposomes which are known to remain intact in the circulating blood. If the possibility that liposomes are bound and/or trapped transiently by blood vessels can be excluded, a gradual increase in the uptake of such liposomes in organs or tissues with time would suggest that the intact liposomes pass out of the vascular system and are taken up by surrounding tissues.

Recent studies on the bovine brain sphingomyelin (SM)/cholesterol (CH) small unilamellar vesicles (SUV) from our laboratory and others indicated that this type of liposome remains intact and retains entrapped substances in the circulating blood of mice with an unusually long half-life of 16-17 hrs. This study investigated the biodistribution of bovine brain sphingomyelin (SM)/cholesterol (CH) (2/1: M/M) small unilamellar vesicles (SUV) in mice, addressing specifically the volume of distribution and transcapillary passage of the SUV.

Figure 5 depicts the percentage of the total administered dose of SM/CH (2/1; M/M) SUV as estimated from the radioactivity of the liposome-encapsulated  $^{111}\text{In}$  present in the vascular system of mice (taking the blood volume, VRBC, as 8.0% of the total body weight) at various periods post-intravenous administration of liposomes. The volume of distribution of the liposomes was found to be

1.28 times VRBC as calculated from the recovery of the administered dose extrapolated to time zero in Figure 5. PAC study of mice sacrificed at 1 min throughout the testing period to 24 hr post-injection indicated that all the In-111 in blood was encapsulated in intact liposomes. Thus, the SM/CH (2/1; M/M) SUV remained intact in the circulating blood and were cleared from the blood slowly. The volume of distribution of the SM/CH SUV was found to be larger than that of red blood cells. There are several possible explanations for this observation.

The most likely possibility is that initially the SM/CH SUV have a larger volume of distribution than red blood cells within the vascular system, which is reasonable since these SM/CH SUV have a diameter approximately 250-fold smaller than erythrocytes. If this is the case, one might anticipate that after the injected liposomes distribute and equilibrate throughout the vascular system, the biodistribution of the SM/CH SUV would remain relatively invariant as long as the liposomes remain intact in the blood circulation. The PAC results clearly indicated that the SM/CH SUV do indeed remain intact in the circulating blood throughout the testing period of 24 hours. However, the results listed in Table 2 indicate that the biodistribution of the SM/CH SUV changes gradually with time. As shown in Table 2, there is a gradual accumulation of liposomal radioactivity in many tissues (eg, skin and intestine), indicating that in addition to the RES system, other tissues participate in the uptake of liposomes.

There are at least two possible explanations which may account for the time-dependent accumulation of liposomes in some tissues listed in Table 2. First, SM/CH SUV bind to the vascular wall rather than distributing to extravascular tissue sites. Second, intact SM/CH SUV pass out of the vascular system and interact with surrounding tissue. If the first explanation were true, one would expect extensive uptake of liposomes at 23 hours post-injection in highly vascularized tissues, such as lung. This was not found to be the case (Table 2). Furthermore, we have shown previously that the SM/CH SUV taken up by liver are degraded rapidly in vivo. Thus, if liposomes were bound to vascular walls and degraded in situ, the release of some liposome-entrapped In-111 into the blood circulation would be expected. It is known that transferrin-bound In-111 remains in the blood circulation for an extended period of time. The result of the PAC study of the blood samples clearly indicated that no In-111 was released or bound to serum proteins during the course of the experiment. Therefore, the most plausible explanation of the gradual accumulation of liposomal radioactivity in certain tissues with time is that intact SM/CH SUV do pass out of the vascular system and gradually accumulate in these tissues, skin and intestine, for example. Furthermore, the extent of the transfer of the SM/CH SUV across capillaries in different tissues is not necessarily the same. This is probably related to the anatomic difference of the intrinsic structure of various classes of capillaries.

In conclusion, the complex of nitrilotriacetic acid with In-111 or Ga-67 ions was encapsulated in the SUV as the radioactive marker for various studies. The structural integrity of liposomes in vitro and in vivo was monitored by the technique of gamma ray perturbed angular correlation. Our data suggested that initially the SM/CH SUV remained within the vascular system and occupied a volume of distribution approximately 1.28 times larger than that of erythrocytes in the vascular system of mice. However, our data also indicated that with time the SM/CH SUV could get out of the vascular system of mice and were taken up

by surrounding tissues over a period of 24 hours. Detailed descriptions of the study are published in a paper in Life Sciences (3).

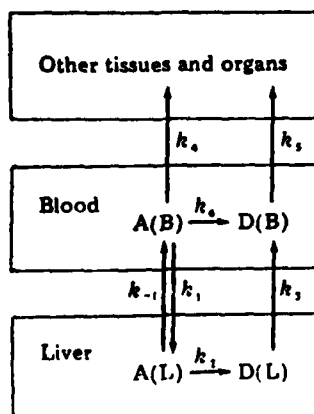
### III. Degradation of liposomes in mouse liver in vivo and in vitro.

The rate and extend of the degradation of drug-loaded liposomes in tissues is a major factor affecting the success of therapy using a drug delivery approach. The characterization of the degradation process of liposomes in tissues is a prerequisite for the rational application of liposomes as a delivery system for therapy or prophylaxis. Furthermore, the response to therapeutic agents delivered by liposomes is directly related to the bioavailability of the encapsulated drug. Therefore, in studying the fate of liposomes in vivo, it is important to establish the tissue distribution of the liposomes as well as the rate and extent of release of the liposome contents.

Using conventional radioactive tracer methods, it is usually difficult to differentiate between radioactivity present in a tissue sample which still remains within intact liposomes and that which has been released from a degraded liposome. This depends on how well the structural integrity of the liposome is maintained in vivo. The physical state or stability of liposomes in vivo is a parameter not readily determinable by current standard techniques. To address this problem, we have developed a simple, general approach combining classical radioactive tracer methods with the technique of PAC to study the fate of liposomes in vivo. This approach involves the encapsulation of the complex of  $^{111}\text{In}^{3+}$  with nitrilotriacetic acid in the aqueous reservoir of liposomes. Conventional radioisotope tracer methods are employed to determine the distribution of liposomes, and the structural integrity of liposomes is monitored by the technique of PAC.

It appears that by combining the data of the structural integrity of liposomes in tissues with the distribution in various organs, the rate constants involved in hepatic uptake and degradation of liposomes may be determined by the approach of least-squares analysis, with an appropriate model. The present study describes the application of a three-compartment model to determine the kinetics of the uptake and degradation of unilamellar liposomes in the liver, assuming first-order kinetics for all rate processes.

The uptake and degradation of liposomes in tissues were analyzed by means of a kinetic model. For simplicity, the body is subdivided into three major compartments: blood, liver, and other organs.



The basic assumption of the analysis is that all rate processes involved are first order. Excretion is not considered in the present model because the renal and fecal excretion of radioactivity is negligible (about 0.5% of the injected dose in a 23-hr period). The amount of intact liposomes, expressed as the percentage of administered dose in the blood and in the liver, is denoted by  $A(B)$  and  $A(L)$ , respectively. The amount of radioactivity released from the degraded liposomes to the circulating blood and the liver is represented by  $D(B)$  and  $D(L)$ , respectively. The hepatic uptake of intact liposomes from the blood is described by a rate constant  $k_1$ , whereas intact liposomes in the liver may return to the blood stream with a rate constant of  $k_{-1}$ . Radioactivity released from the degraded liposomes in the liver may return to the circulating blood with a rate constant of  $k_3$ . The uptake of intact liposomes and the uptake of the radioactivity released from degraded liposomes by other tissues and organs are denoted by rate constants of  $k_4$  and  $k_5$ , respectively. The degradation of liposomes in the liver and in the blood is designated by rate constants of  $k_2$  and  $k_6$ , respectively.

Based upon the model, the rate equations for the four observed parameters of the radioactivity of intact and degraded liposomes in the circulating blood and liver are shown below.

$$\begin{aligned} dA(B)/dt &= -k_1(A(B)) + k_{-1}(A(L)) \\ &\quad - k_4(A(B)) - k_5(A(B)) \\ dA(L)/dt &= k_1(A(B)) - k_{-1}(A(L)) - k_2(A(L)) \\ dD(L)/dt &= k_2(A(L)) - k_3(D(L)) \\ dD(B)/dt &= k_3(D(L)) - k_3(D(B)) + k_6(A(B)) \end{aligned}$$

The solutions at any time  $t$  were obtained by means of the IMSL (International Mathematical and Statistical Library) subroutine, DVERK, which uses a Runge-Katta method based on Vernier fifth-and-sixth-order pairs of formulas. From these solutions, the total amounts of radioactivity in the blood and in the liver and the time-integrated perturbation factor of the excised liver samples could be calculated. In calculating the  $\langle G_{22}(\infty) \rangle$  values, the following equation was used:

$$\langle G_{22}(\infty) \rangle_t = X_t \langle G_{22}(\infty) \rangle_{\text{intact}} + (1-X_t) \langle G_{22}(\infty) \rangle_{\text{degraded}},$$

in which  $X_t$  represents the percentage of intact vesicles in the liver at the time  $t$  after injection. The  $\langle G_{22}(\infty) \rangle$  values, 0.59 and 0.12, corresponding to intact and completely disrupted vesicles, respectively, were used. These theoretical results were compared with the corresponding experimentally measured data at various times after injection. To simplify our analysis, SM/CH liposomes were used, since they remained intact in circulating blood for at least 24 hr. Because of this, the rate constant for liposomal degradation in the blood,  $k_6$ , was set at zero and was not varied. The other rate constants were then varied systematically until the sum of the squares of the deviation between the corresponding experimental and theoretical values was minimized. The instantaneous hepatic degradation rate of liposomes was evaluated by means of the final set of rate constants determined by the above least-squares fitting program with no weighting function.

To determine the *in vitro* hepatic degradation rate of liposomes in the excised liver sample at 37°C, we assumed the same kinetic model, whereas only the experimental PAC data were used in the fitting analysis. All computations were performed by means of the CDC 6400 computer system, maintained by the



Academic Computer Center of the University of Washington.

Based upon the model described above and the least-squares kinetic analysis, the rate constants of the various processes of uptake and degradation of liposomes are shown in Table 3. It should be pointed out that the reporter molecule,  $^{111}\text{In}^{3+}$ , was loaded into only the outermost aqueous compartment of the multilamellar liposomes. The degradation of the lipid bilayer for small unilamellar and large multilamellar liposomes is thus comparable. The average size of the SM/CH SUV was  $187 \pm 42$  Å in diameter, and the minimal size of the SM/CH MLV in the present study was larger than the pore-size of the Sepharose 4B gel.

Four observations may be made from an examination of the data in Table 3. First, because of the difference in the size distribution of the three different preparations of the large multilamellar liposomes, the rate constant of the uptake of these liposomes by the liver ( $k_1$ ) varies. Second, in contrast to the small unilamellar liposomes, the large multilamellar liposomes are taken up rapidly by the liver as indicated by the high values of  $k_1$ . Third, despite the variation in  $k_1$  among the large multilamellar liposomes, the rate constants for the degradation of these large liposomes in the liver ( $k_2$ ) are not very different. Fourth, the average half-life ( $t_{1/2} = 0.693/k_2$ ) of the in vivo degradation of the small unilamellar liposomes ( $3.55 \pm 0.25$  hr) is significantly longer than that of the large multilamellar liposomes ( $1.38 \pm 0.22$  hr).

By using the rate constants in Table 3, it was possible to predict the total amount of radioactivity from intact and degraded liposomes present in the blood and the liver and the  $\langle G_{22}(\infty) \rangle$  values of the liver. Figure 6 depicts the fit between the experimental observations and the predicted values of two typical preparations of small and large liposomes, respectively.

The high  $\langle G_{22}(\infty) \rangle$  values of the livers excised from mice killed 15 min after injection indicated that little degradation had occurred at that early time point. The continuing in vitro degradation of liposomes in the excised liver could be followed by monitoring the change of the  $\langle G_{22}(\infty) \rangle$  values. The percentage of intact liposomes that remained in the liver can then be determined by Eq. 1. The in vitro degradation of the SM/CH SUV in a single liver sample with time at two different temperatures is depicted in Fig 7. The rate of degradation of SUV in liver decreased as the temperature decreases. This may imply that the degradation is an enzymatic process. The kinetic analysis of the rate of the release of  $^{111}\text{In}^{3+}$  from SUV in the liver at  $37^\circ\text{C}$  (Fig. 7) suggests that hepatic degradation of SUV follows first-order kinetics with a half-life of  $3.5 \pm 0.2$  hr., which is very similar to the in vivo result of  $t_{1/2} = 3.55 \pm 0.25$  hr. In contrast, the relative rates of degradation of the outermost bilayer of large multilamellar liposomes of the same composition in the liver was very different in the in vitro and in vivo situations (Fig. 8). As can be estimated from Figure 8, the half-life of the in vitro degradation of the outermost shell of the large bath-sonicated liposomes is 8-9 hrs, which is about 6 times longer than the  $t_{1/2}$  of 1.38 hr. calculated from the average  $k_2$  of the same type of liposomes in Table 3. Our results indicated that the phenomenon of the retarded degradation of large liposomes in vitro was not restricted to bath-sonicated multilamellar liposomes. Figure 9 depicts the time course of the in vitro degradation of a typical bovine brain sphingomyelin/cholesterol (2:1; mol/mol) multilamellar liposome prepared by extrusion (18).

In conclusion, the rate of degradation of liposomes in mouse liver is affected by the size of liposomes. It was found that in the liver the outermost lipid bilayer of the large multilamellar liposomes was degraded more rapidly than the bilayer of the small unilamellar liposomes in vivo. Our results suggest that multiple pathways operate in the degradation of liposomes in the liver. Some of the results described in this section have been published in a paper in *Prod. Natl. Acad. Sci. USA* (4) and in a manuscript to be submitted to *Biochim. Biophys. Acta* for publication (5)

#### IV. The long half-life of blood clearance of SM/CH (2/1; mol/mol) SUV in mice.

The uptake of liposomes by the reticuloendothelial system is the major cause of the elimination of liposome-entrapped drugs from the circulation. Some large liposomes could be removed from the circulation in the first few passages through the liver. Thus, in order to achieve the goal of targeting liposome-entrapped drugs to desired tissues or organs, it is important to prolong the presence of intact liposomes in the blood.

One of the most exciting findings of our research in the search for liposomes with a long half-life of blood clearance was the initial discovery of intact SM/CH (2/1; mol/mol) SUV remaining in the circulating blood of mice with a half-life of about 16.5 hr. This is the longest clearance time ever reported for liposomes of natural sources. Subsequent study of the influence of various factors on the clearance of SM/CH SUV indicated that the kinetics of the elimination of the SM/CH (2:1; mol/mol) small unilamellar vesicles from the blood was markedly affected by the amount of the administered liposomal lipid. Figure 10 depicts the blood clearance of liposomally entrapped In-111 in "low" and "high" liposomal lipid dose ranges over time. A "low" liposome dose was arbitrarily defined as injected dose less than 20  $\mu$ g lipid per g body weight, and a "high" liposome dose was taken as dose greater than 53  $\mu$ g lipid per g body weight. The patterns of the elimination of these two dose levels are essentially the same to 3-5 hours post-injection of the SM/CH vesicles. However, at later time points post-injection of the SM/CH vesicles, the effect of lipid dose has quite a significant influence on the pattern of the elimination of the liposomes from the blood.

Figure 11 illustrates the dependency of the percentage of the total administered liposomally entrapped In-111 present in the blood or liver on the dose of administered liposomal lipid at 23 hours post-injection. The dose dependency was examined over a lipid dose range of 3 to 316  $\mu$ g total lipid per g mouse body weight. At a lipid dose of approximately 120  $\mu$ g/g, a plateau level of 40% of the administered dose is achieved in the blood. This 40% level remains invariant over the dose range examined to 316  $\mu$ g/g at 23 hours post-administration. An inverted pattern is evident from an examination of the percentages present in the liver over the same lipid dose range. Apparently, beyond the 120  $\mu$ g/g threshold lipid dose level, saturating doses have been attained and the liver uptake accounts for a constant 20% of the administered liposomal lipid dose at 23 hours post-injection. This pattern suggests two parallel hepatic uptake processes: one which is saturable over the dose range studied and another which is not.

In conclusion, the SM/CH (2/1; mol/mol) SUV ( $187 \pm 42$  nm in diameter) remain intact in the vascular system of a mouse with a half-life of blood elimination of up to 24 hours, depending upon the dose of lipid administered. This is considerably longer than the half-lives reported by phosphatidylcholine/cholesterol liposomes in the literature. Our initial finding has been published in a paper in *Proc. Natl. Acad. Sci. USA* (4). A manuscript describing the effect of lipid dose has been submitted to *Biochim. Biophys. Acta* for publication (6)

## REFERENCES

1. Hwang, K. J., Merriam, J. E., Beaumier, P. L. and Luk, F-K. S.: Encapsulation, Encapsulation, with high efficiency, of radioactive metal ions in liposomes. *Biochim. Biophys. Acta* 716:101-109, 1982.
2. Beaumier, P. L. and Hwang, K. J.: An efficient method for loading indium-<sup>111</sup> into liposomes using acetylacetone. *J. Nucl. Med.* 23: 810-815 , 1982.
3. Hwang, K. J., Luk, K-F. S., and Beaumier, P. L.: Volume of distribution and transcapillary passage of small unilamellar vesicles. *Life Sciences* 31:949-955, 1982.
4. Hwang, K. J., Luk, K-F. S., and Beaumier, P. L.: Hepatic Uptake and degradation of unilamellar sphingomyelin/cholesterol liposomes: a kinetic study. *Proc. Natl. Acad. Sci. USA.* 77:4030-4034, 1980.
5. Beaumier, P. L. and Hwang, K. J.: Effects of liposome size on the liver degradation of bovine brain sphingomyelin/cholesterol liposomes in mouse liver. *Biochim. Biophys. acta.* manuscript in preparation, 1982.
6. Beaumier, P. L., Hwang, K. J., and Slattery, J. T.: Effect of liposome dose on the elimination of small unilamellar sphingomyelin/cholesterol vesicles from the circulation *Biochim. Biophys. Acta.* Submitted for publication, 1982.

## LEGENDS OF FIGURES

- Figure 1. Dependence of the loading efficiency of (a)  $^{111}\text{In}^{3+}$  and (b)  $^{67}\text{Ga}^{3+}$  into DPPC small unilamellar liposomes on the concentration of oxine (o-o) or oxine sulfate (e-e). The DPPC liposomes entrapping 0.106M sodium phosphate, pH 7.4, 1mM NTA was in 0.9% NaCl, 5mM sodium acetate, pH 5.5, at a concentration of 10-15 mg/ml lipid. The percentage of loading was determined by the ratio of the radioactivity of  $^{111}\text{In}^{3+}$  or  $^{67}\text{Ga}^{3+}$  associated with liposomal fractions after AGIX-8 chromatography to the total radioactivity of oxine- $^{111}\text{In}^{3+}$  (or  $^{67}\text{Ga}^{3+}$ ) in the incubation mixture of liposomes and oxine-metal. Each point is an average of two measurements for In-111 and three measurements for Ga-67.
- Figure 2. The dependence of loading efficiency of the concentration of acac used to introduce In-111 into SM/CH (2/1; mol/mol) SUV. The loading efficiency was estimated from the ratio of the radioactivity which emerged from the AG 1-X8 column to the total radioactivity overlaid. Each point is the average of three measurements.
- Figure 3. Dependence of the loading efficiency of  $^{111}\text{In}^{3+}$  into DSPC/CH (2/1; mol/mol) small unilamellar liposomes on the pH. Oxine (o-o) and oxine sulfate (e-e) were to load  $^{111}\text{In}^{3+}$  into liposomes as described in the legend of Figure 1 except that that the liposomes encapsulated 0.9% NaCl, 1mM NTA, pH 7.4. Each point is an average of two measurements.
- Figure 4. Effect of citrate on the efficiency of loading  $^{111}\text{In}^{3+}$  to DPPC small unilamellar liposomes. Oxine was used to load  $^{111}\text{In}^{3+}$  into liposomes as described in the legend of Figure 1. The concentration of citrate was adjusted by mixing the liposomes suspension with an appropriate volume of 0.129 M sodium citrate, pH 5.5. Each point is an average of two measurements.
- Figure 5. Clearance of SM/CH (2/1; mol/mol) SUV from the blood of mice. The percentage of injected liposomes in the blood was calculated from the specific activity of the liposome-entrapped In-111 in the blood and an average blood volume of 8.0% of the body weight. The number of animals for each point were 3, 8, 3, 6, and 10 at 1, 15, 30, 60, and 180 minutes post-injection, respectively. The dotted line is the extrapolation of the straight line of 15, 30, 60, and 180 minutes to the zero time. The zero time activity was estimated to be 78% of the injected liposomes.
- Figure 6. Blood clearance, liver uptake, and the in vivo hepatic degradation of liposomes. The liposomes were bovine brain sphingomyelin/cholesterol (2:1;mol/mol) small unilamellar liposomes (left frame) and bath-sonicated large multilamellar liposomes (right frame). The percentage of intact liposomes in the liver is plotted at the right coordinate and the half-life of the in vivo degradation of each type of liposome is shown in the lower figure of each frame. The observed values are denoted by (●) and the calculated values are represented by the lines.

- Figure 7. In vitro degradation of SM:CH (2/1; mol/mol) SUV in an excised liver at two different temperatures. The liver was removed from a mouse sacrificed at 15 minutes post-administration of liposomes. The  $\langle G_{22}(\infty) \rangle$  values of the liver sample were measured at 37°C (X) and 24°C (Δ). The predicted  $\langle G_{22}(\infty) \rangle$  values (0-0) were calculated using an equation (1) and the first order in vitro rate constant,  $k_2 = 0.2$ . The percentage of intact liposomes corresponding to the  $\langle G_{22}(\infty) \rangle$  values is shown on the right axis.
- Figure 8. Degradation of the outermost shell of bovine brain sphingomyelin/cholesterol (2:1; mol/mol) bath-sonicated large multilamellar liposomes in the liver in vitro and in vivo. Three different preparations of liposomes were used for the in vitro study (O, □, Δ). Two different preparations of liposomes were used for the in vivo study (●, ■). In the in vivo study, each point represents the  $\langle G_{22}(\infty) \rangle$  of one excised liver.
- Figure 9. In vitro degradation of the outermost shell of bovine brain sphingomyelin/cholesterol (2:1; mol/mol) membrane-extruded large multilamellar liposomes in two different livers.
- Figure 10. The clearance of SM/CH (2/1; mol/mol) small unilamellar vesicles from the blood of BALB/c mice at two typical liposome doses. Low liposome dose (●-●) was taken as injected dose less than 20 ug lipid per g body weight. Each point is the average of at least six measurements. High liposome dose (O-O) was chosen as dose above 53 ug lipid per g body weight. Except for the point at 23 hours, all the points represent one or the average of two measurements.
- Figure 11. The effect of liposome dose on blood clearance and liver uptake of SM/CH small unilamellar vesicles at 23 hours post-injection. (Δ-Δ) designates percentages of injected liposomes remaining in the blood and (●-●) designates percentages of injected liposomes accumulated in the liver.

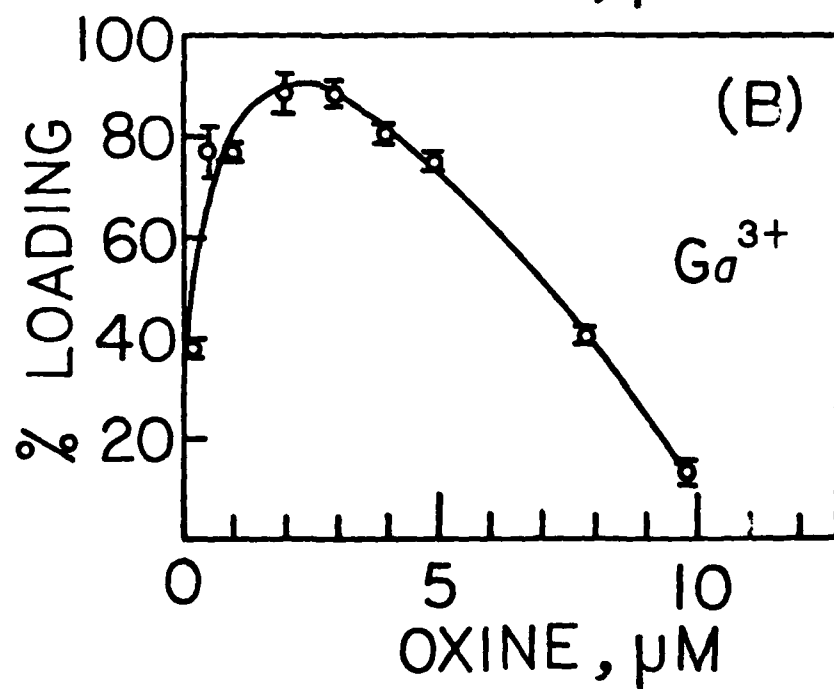
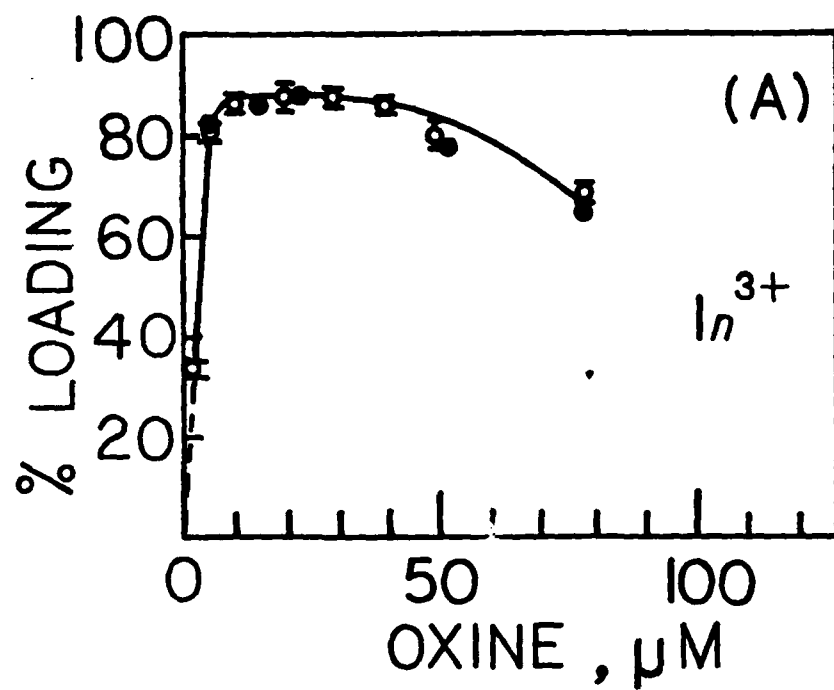


Figure 1

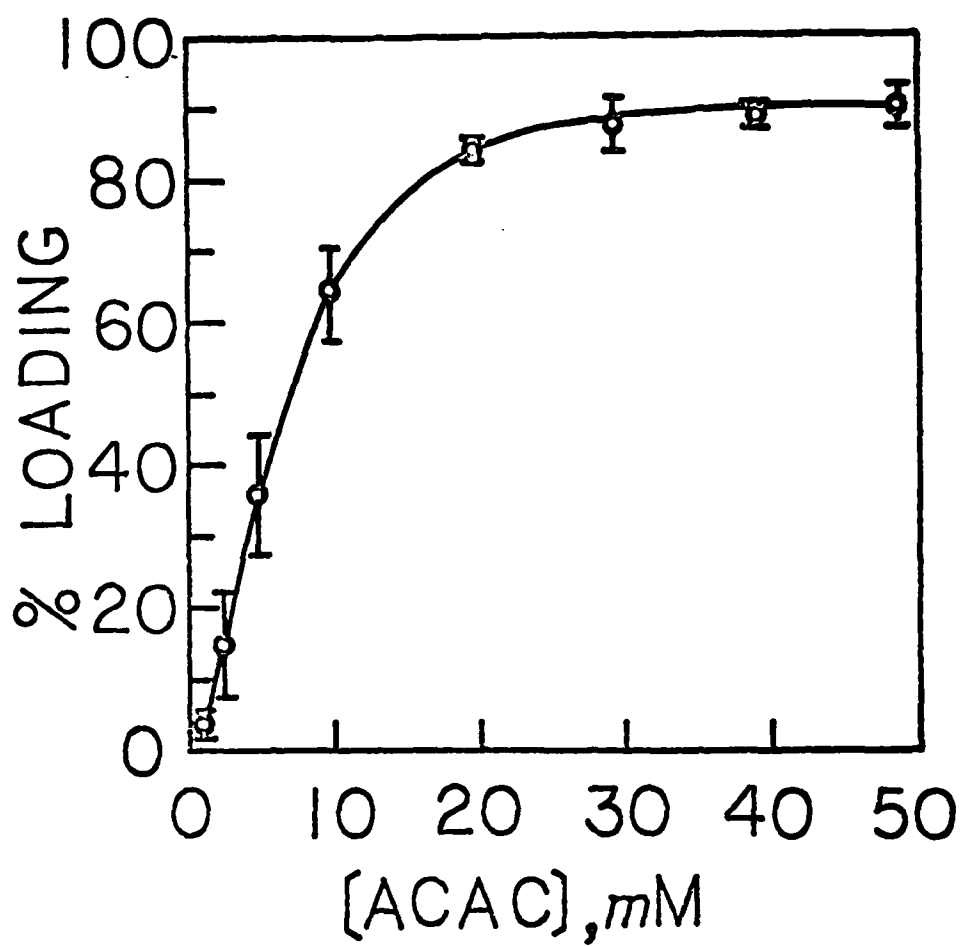


Figure 2

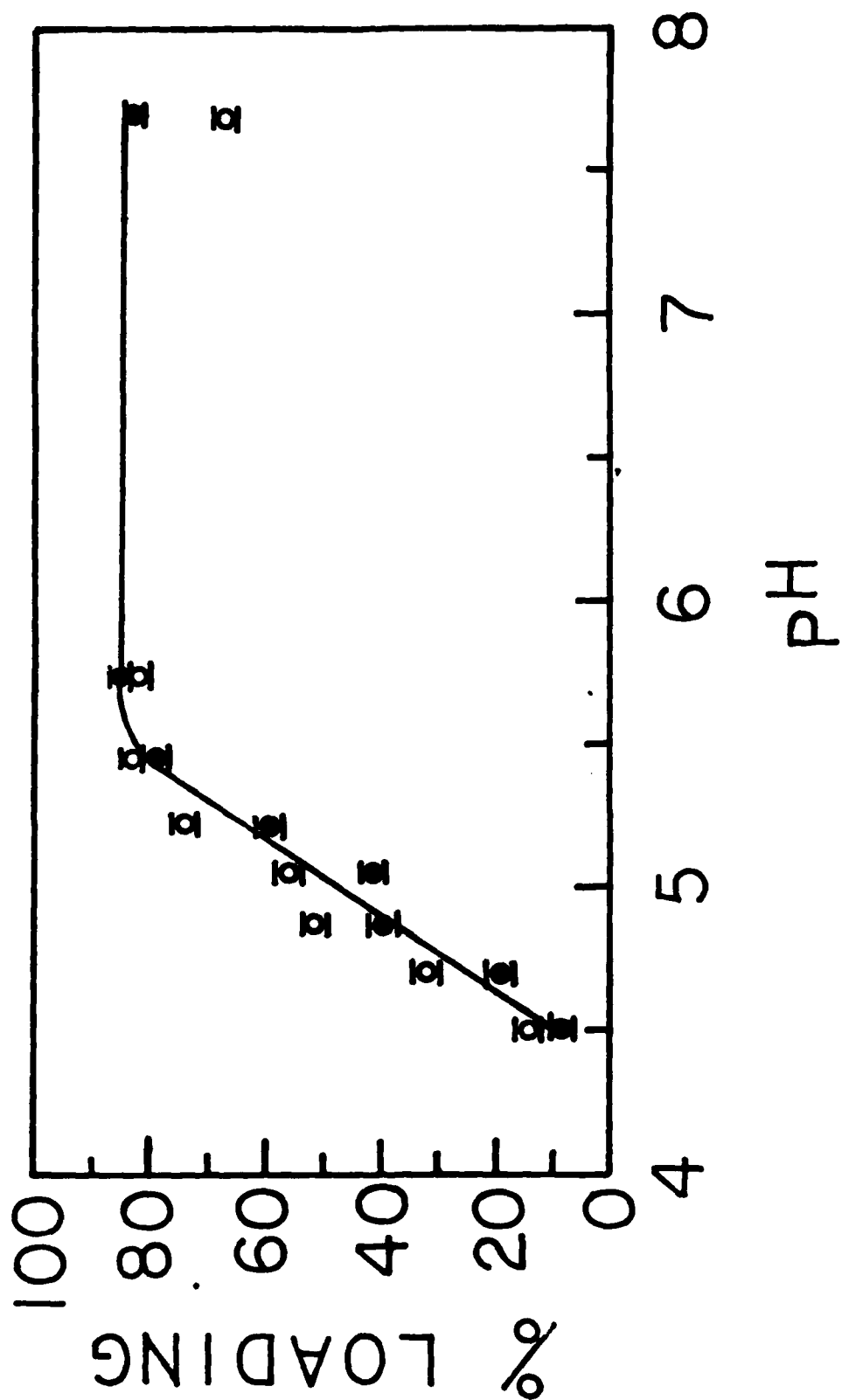


Figure 3



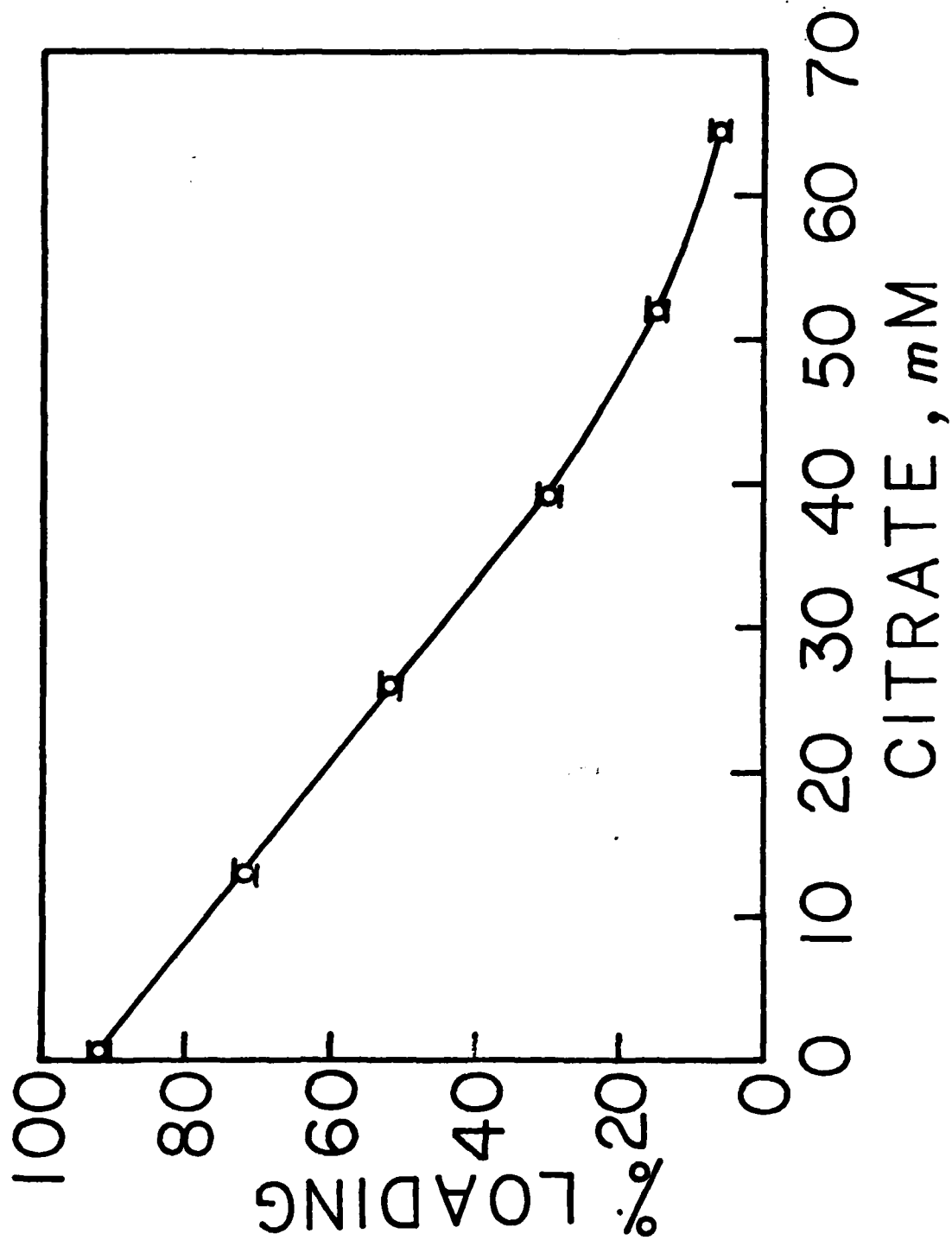


Figure 4

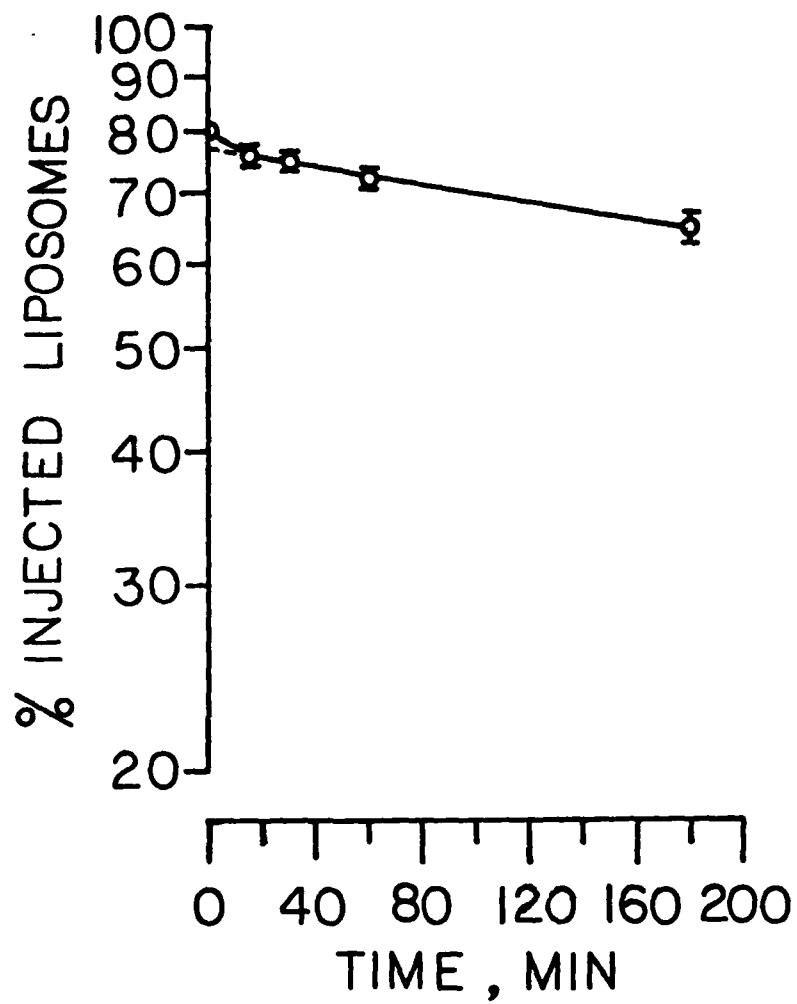


Figure 5

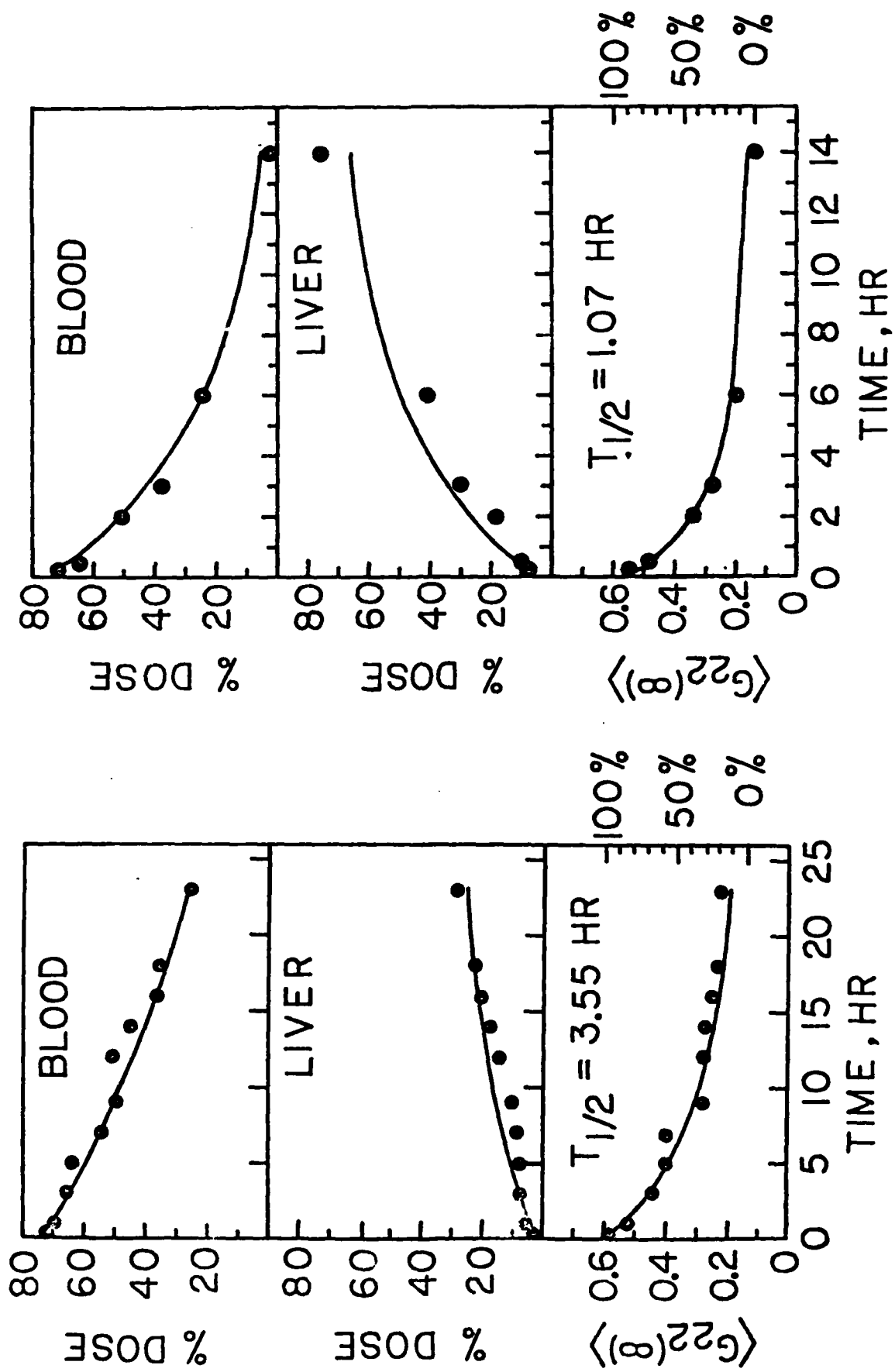


Figure 6

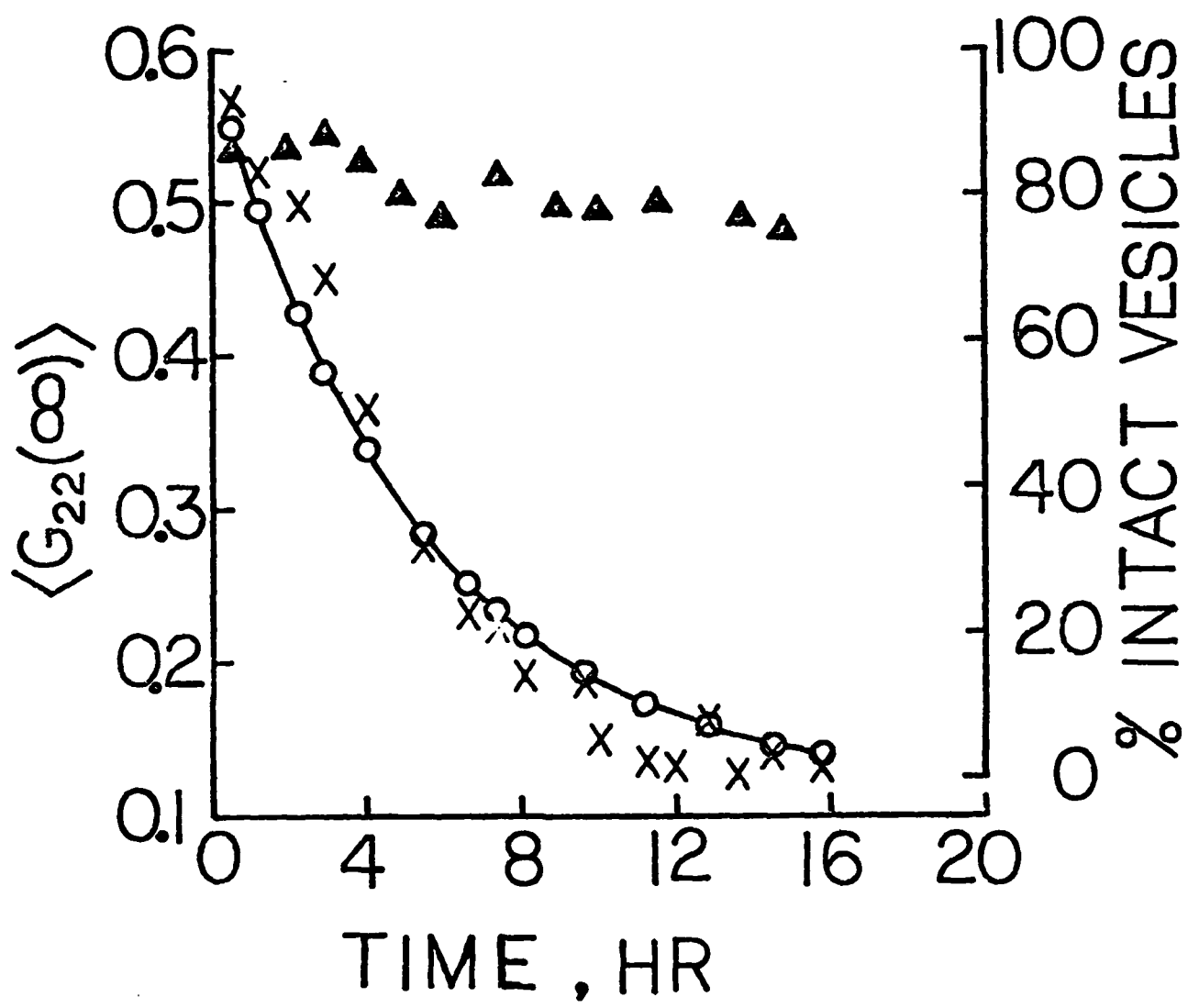


Figure 7

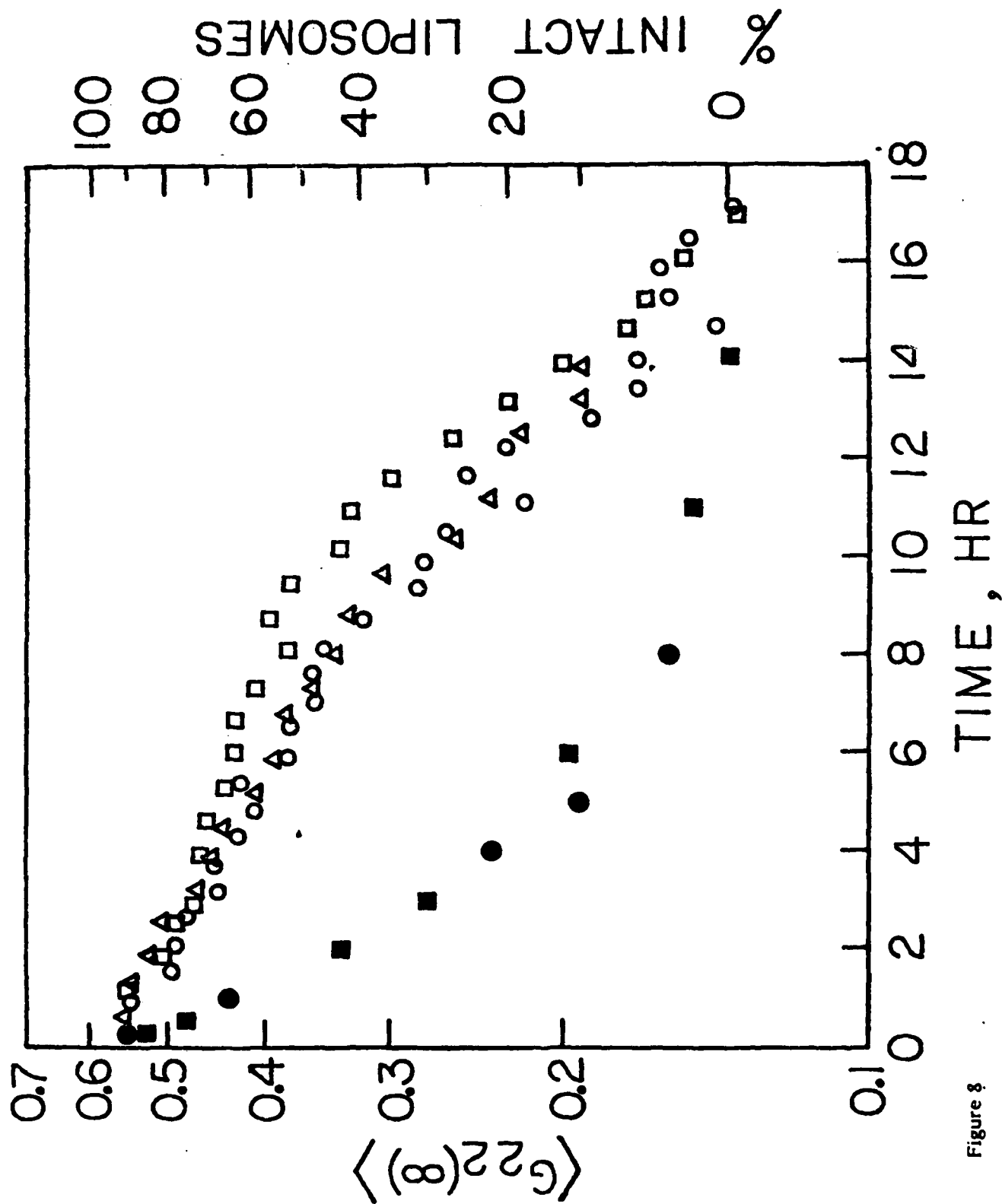


Figure 8

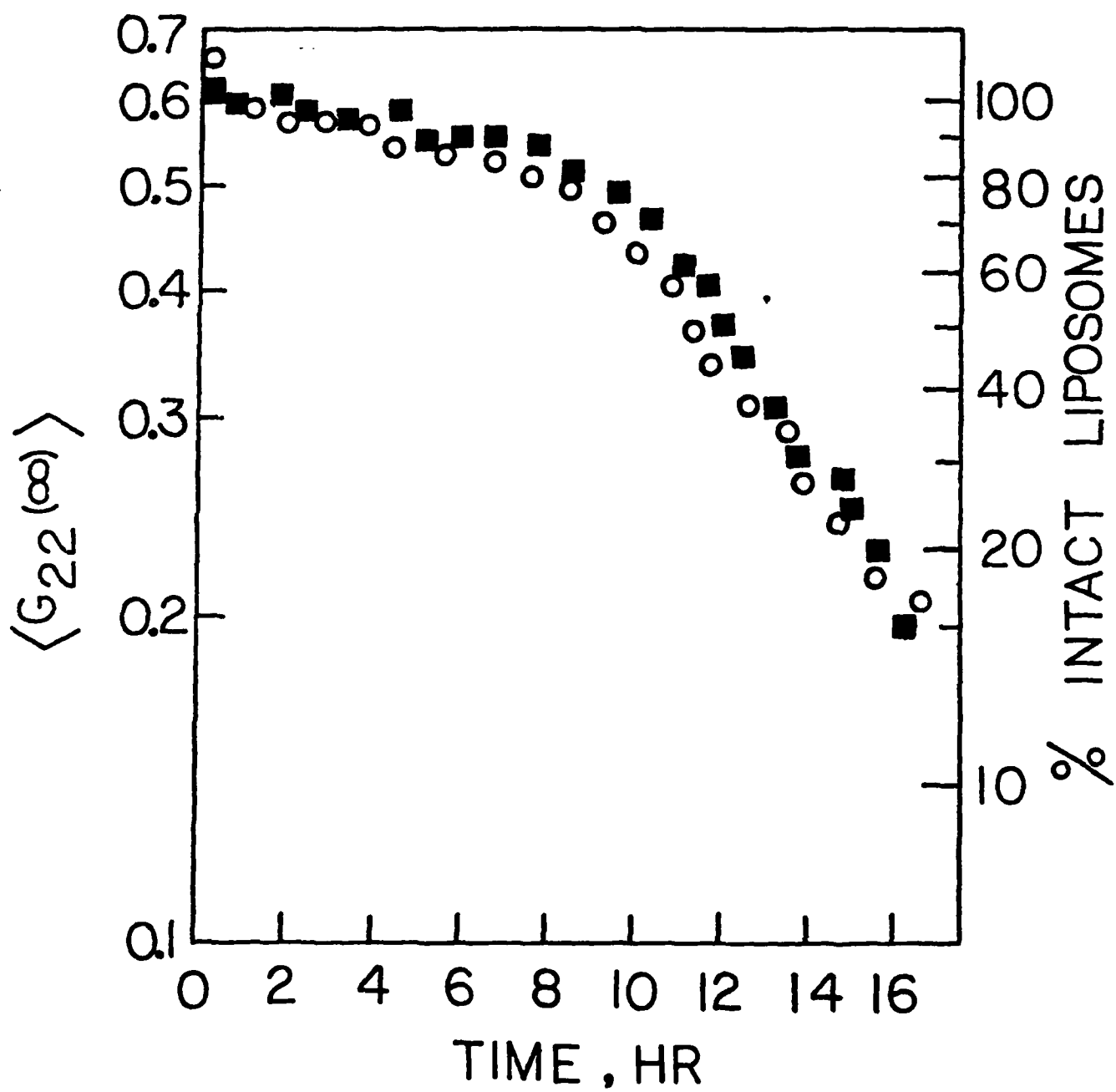


Figure 9

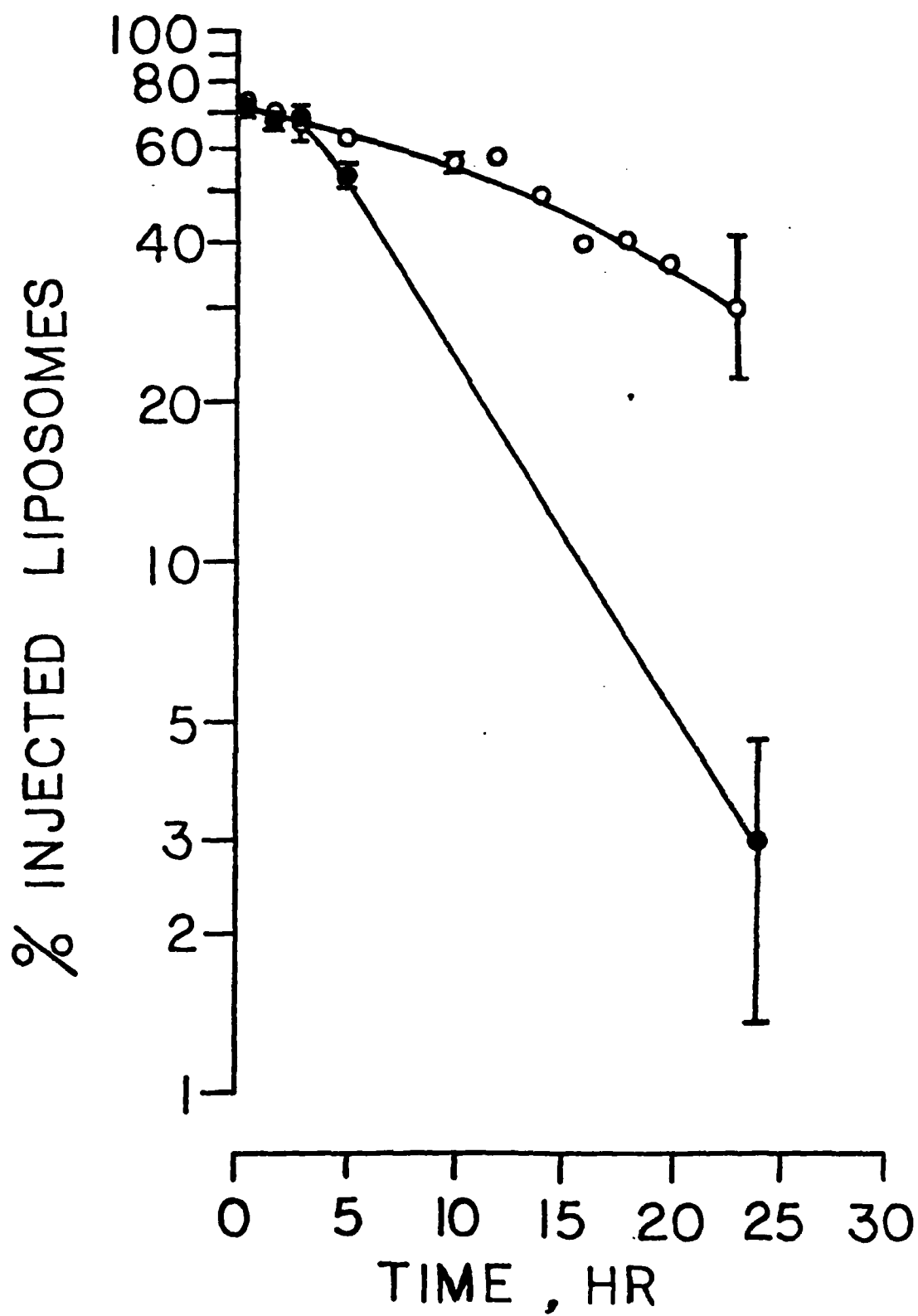


Figure 10

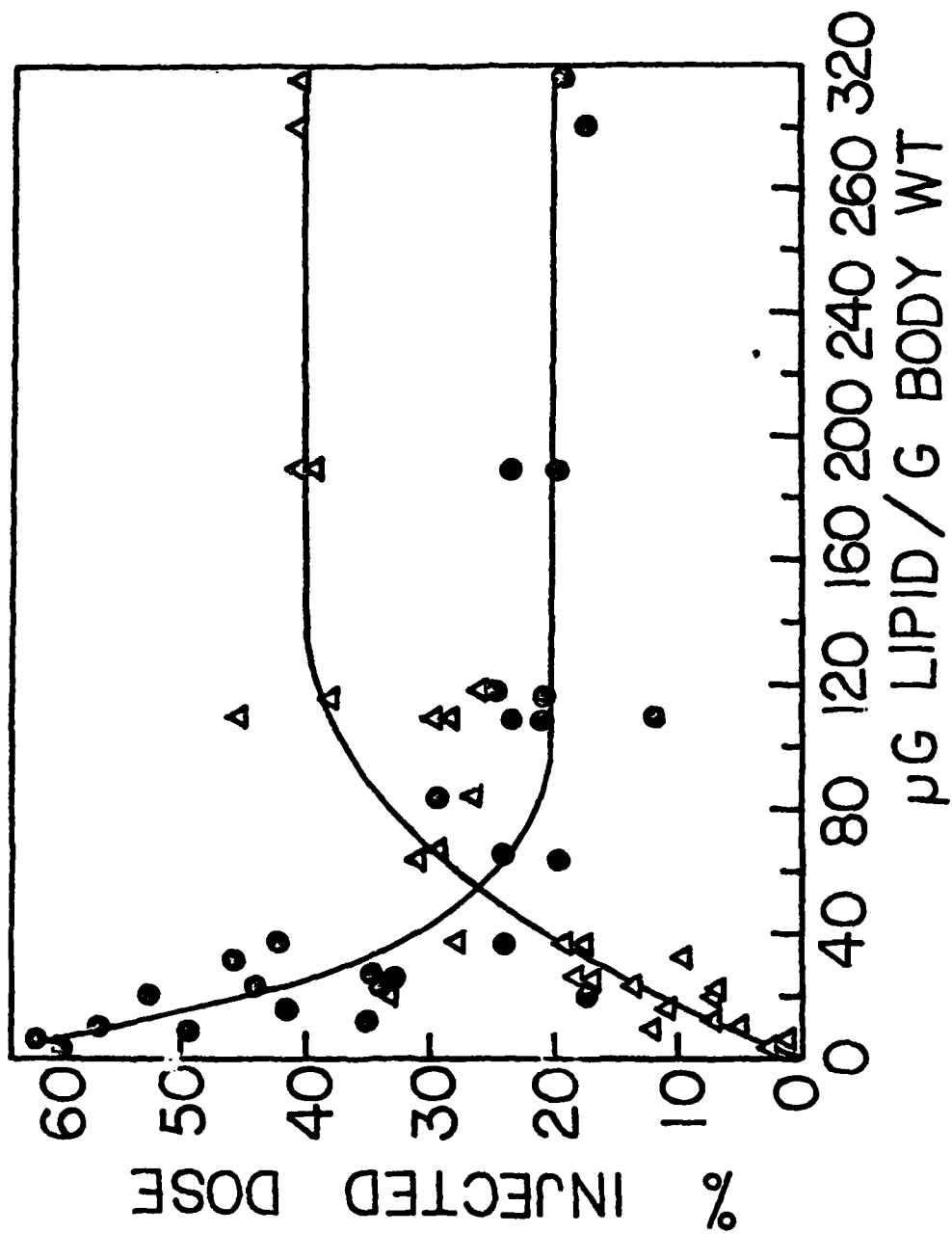


Figure II



TABLE 1.

Tissue Distributions of Unilamellar SM:CH (2/1; M/M) Liposomes Entrapping Ga-67 by Sonication and the same type of Liposomes Entrapping In-111 by In-111-oxine loading in mice\*

	<u>1 hr.</u>		<u>3 hr.</u>		<u>23 hr.</u>	
	Ga-67	In-111	Ga-67	In-111	Ga-67	In-111
Blood	69.2(2.7)	70.5(2.2)	64.4(0.2)	65.5(0.3)	29.6(1.2)	26.8(0.1)
Liver	5.4(0.7)	4.9(0.8)	7.9(1.0)	7.9(1.0)	24.3(1.2)	29.6(0.9)
Kidney	0.9(0.0)	1.1(0.1)	0.9(0.0)	1.1(0.1)	2.1(0.0)	2.1(0.0)
Spleen	0.2(0.1)	0.2(0.1)	0.4(0.1)	0.4(0.1)	1.5(0.0)	1.9(0.1)
Heart	0.2(0.1)	0.2(0.2)	0.0(0.0)	0.0(0.0)	0.3(0.1)	0.4(0.1)
Lung	2.7(2.7)	2.6(2.2)	0.6(0.2)	0.6(0.1)	2.1(0.1)	1.9(0.3)
Intestine	2.4(0.1)	2.2(0.1)	3.4(0.3)	3.0(0.3)	8.7(0.8)	7.1(0.9)
Fat	0.7(0.1)	0.8(0.0)	1.3(0.1)	1.2(0.1)	1.0(0.1)	0.9(0.1)
Skin	2.6(0.3)	2.4(0.4)	4.8(0.5)	4.5(0.4)	9.5(0.2)	10.7(0.1)
Tail	4.3(0.8)	4.3(0.6)	3.3(0.1)	3.3(0.1)	3.1(0.3)	3.0(0.2)
Legs	2.1(0.3)	2.0(0.3)	3.2(0.2)	3.0(0.1)	5.8(0.4)	5.4(0.3)
Carcass	8.7(0.7)	8.3(0.5)	9.4(0.8)	9.1(0.8)	11.0(0.2)	9.3(0.0)
Brain	0.2(0.0)	0.3(0.0)	0.2(0.0)	0.2(0.0)	0.1(0.0)	0.1(0.0)
Stomach	0.3(0.0)	0.2(0.1)	0.3(0.1)	0.3(0.1)	0.8(0.0)	0.8(0.1)

\*About 1.8mg lipids was injected to each mouse in a volume of 100  $\mu$ l by intravenous injection. The number in the parenthesis is the average deviation from the mean of two independent measurements.

TABLE 2

Time Course of Biodistribution of Injected Liposomal Radioactivity in Mice\*

Tissue	Percentage ( $\pm$ SD) of Administered Dose at Various Times After Injection				
	1 Min (N=3)	15 Min (N=8)	1 Hr (N=6)	3 Hr (N=10)	23 Hr (N=6)
Blood	80.0(0.2)	75.1(2.1)	72.5(2.3)	64.8(1.9)	15.7(7.2)
Liver	2.8(0.3)	4.9(0.2)	5.4(1.0)	7.3(1.2)	44.3(8.0)
Kidney	1.0(0.0)	1.0(0.1)	1.3(0.4)	1.5(0.2)	2.1(0.6)
Spleen	0.0(0.0)	0.0(0.0)	0.0(0.0)	0.3(0.2)	1.8(0.1)
Heart	0.0(0.0)	0.4(0.1)	0.4(0.4)	0.6(0.2)	0.4(0.3)
Lung	3.6(1.9)	2.3(0.6)	1.7(9.7)	1.8(1.7)	1.0(0.4)
Intestine	0.7(0.0)	1.4(0.2)	1.8(0.9)	3.0(0.3)	5.7(1.2)
Fat	0.4(0.3)	0.3(0.1)	0.5(0.3)	0.5(0.1)	1.2(0.6)
Skin	1.7(0.7)	2.4(1.0)	2.9(0.3)	4.2(0.9)	9.3(2.7)
Tail	1.0(0.6)	2.3(0.3)	2.0(0.9)	1.9(0.5)	2.2(0.5)
Legs	2.0(0.4)	2.0(0.2)	3.1(0.7)	2.9(0.3)	4.9(0.8)
Carcass	6.5(1.2)	8.5(1.5)	8.0(3.1)	10.8(0.9)	10.7(2.3)
Brain	0.2(0.1)	0.2(0.0)	0.2(0.1)	0.1(0.1)	0.1(0.0)
Stomach	0.1(0.1)	0.1(0.0)	0.1(0.1)	0.3(0.0)	0.6(0.1)

\*The liposomes were SM/CH (2/1; M/M) SUV entrapping In-111, and N is the number of animals. The lipid dose administered in 100  $\mu$ l ranged from 35 to 75  $\mu$ g total lipid per g mouse body weight. Since In-111 ions bind tightly to tissues at the site of the destruction of liposomes and do not redistribute readily to other tissues, only about 0.5% of the injected dose of In-111 was excreted in a 23-hr period, resulting in a nearly complete recovery of the label after 23 hr.

TABLE 3: Calculated Rate Constants\*

Rate Constant (1/hr)	Small Unilamellar Liposomes	<u>Large Multilamellar Liposomes</u>		
		Set 1	Set 2	Set 3
$k_1$	$0.024 \pm 0.005$	1.280	0.160	1.350
$k_{-1}$	$0.016 \pm 0.016$	0.000	0.000	0.000
$k_2$	$0.195 \pm 0.015$	0.460	0.645	0.450
$k_4$	$0.023 \pm 0.003$	0.000	0.030	0.000

\* The rate constants were obtained by fitting all of the data tissue distribution and the in vivo degradation of In-111-loaded sphingomyelin/cholesterol (2:1; mol/mol) liposomes. The rate constants of small unilamellar liposomes were calculated from the average of two independent data. The rate constants of three different preparations of bath sonicated large multilamellar liposomes are listed separately because of the lack of similarity in their  $t_{1/2}$  of blood clearance and the time course of tissue distribution.

## GLOSSARY

CH:	Cholesterol
DPPC:	L- $\alpha$ -dipalmitoyl phosphatidylcholine
DPPE:	L- $\alpha$ -dipalmitoyl phosphatidylethanolamine
DSPC:	L- $\alpha$ -disteroyl phosphatidylcholine
EDTA:	Ethylenediamine-N,N,N',N'-tetraacetic acid
$\langle G_{22}(\infty) \rangle$ :	Time-integrated perturbation factor. This is the parameter measured by the counters of gamma-ray perturbed angular correlation spectrometer. The value of $\langle G_{22}(\infty) \rangle$ has a range from 0.0 to 1.0. In the system of liposomes, a low value of $\langle G_{22}(\infty) \rangle$ closed to 0.0 means that the liposomes are greatly perturbed and release their encapsulated contents. On the other hand, intact liposomes have a characteristic high $\langle G_{22}(\infty) \rangle$ of about 0.60.
MLV:	Multilamellar vesicles
NTA:	Nitrilotriacetic acid
PAC:	perturbed angular correlation
RES:	Reticuloendothelial system
VRBC:	Blood volume or volume distribution of erythrocytes
SM:	Bovine brain sphingomyelin
SUV:	Small unilamellar vesicles

Personnel Receiving Contract Support

Karl J. Hwang

K-F, Steven Luk

Paul L. Beaumier (Ph.D. received in 1982)

Janet Merriam

Janet Hudkins

Peter Klein

Henry Leung

Jonh H. Wiessner

Janet Gumprecht

Frona Woods

Toni Bukowski

DISTRIBUTION LIST

Director  
Walter Reed Army Institute of Research  
Walter Reed Army Medical Center  
ATTN: SGRD-UWZ-C  
Washington, DC 20307-5100

Commander  
US Army Medical Research and Development Command  
ATTN: SGRD-RMS  
Fort Detrick, Frederick, Maryland 21701-5012

Defense Technical Information Center (DTIC)  
ATTN: DTIC-DDAC  
Cameron Station  
Alexandria, VA 22304-6145

**END**

**FILMED**

**11-84**

**DTIC**